

# Bayesian GAN

Yunus Saatchi  
Amplify Technologies and Permutation Ventures  
saatchi@cantab.net

Andrew Gordon Wilson  
Cornell University  
andrew@cornell.edu

## Abstract

Generative adversarial networks (GANs) can implicitly learn rich distributions over images, audio, and data which are hard to model with an explicit likelihood. We present a practical Bayesian formulation for unsupervised and semi-supervised learning with GANs, in conjunction with stochastic gradient Hamiltonian Monte Carlo to marginalize the weights of the generator and discriminator networks. The resulting approach is straightforward and obtains good performance without any standard interventions such as feature matching, or mini-batch discrimination. By exploring an expressive posterior over the parameters of the generator, the Bayesian GAN avoids mode-collapse, produces interpretable candidate samples with notable variability, and in particular provides state-of-the-art quantitative results for semi-supervised learning on benchmarks including SVHN, CelebA, and CIFAR-10, outperforming DCGAN, Wasserstein GANs, and DCGAN ensembles.

## 1 Introduction

Learning a good generative model for high-dimensional natural signals, such as images, video and audio has long been one of the key milestones of machine learning. Powered by the learning capabilities of deep neural networks, generative adversarial networks (GANs) (Goodfellow et al., 2014) and variational autoencoders (Kingma and Welling, 2013) have brought the field closer to attaining this goal.

GANs transform white noise through a deep neural network to generate candidate samples from a data distribution. A discriminator learns, in a supervised manner, how to tune its parameters so as to correctly classify whether a given sample has come from the generator or the true data distribution. Meanwhile, the generator updates its parameters so as to fool the discriminator. As long as the generator has sufficient capacity, it can approximate the CDF inverse-CDF composition required to sample from a data distribution of interest. Since convolutional neural networks by design provide reasonable metrics over images (unlike, for instance, Gaussian likelihoods), GANs using convolutional neural networks can in turn provide a compelling implicit distribution over images.

Although GANs have been highly impactful, their learning objective can lead to *mode collapse*, where the generator simply memorizes a few training examples to fool the dis-

criminator. This pathology is reminiscent of maximum likelihood density estimation with Gaussian mixtures: by collapsing the variance of each component we achieve infinite likelihood and memorize the dataset, which is not useful for a generalizable density estimate. Moreover, a large degree of intervention is required to stabilize GAN training, including feature matching, label smoothing, and mini-batch discrimination (Radford et al., 2015; Salimans et al., 2016). To help alleviate these practical difficulties, recent work has focused on replacing the Jensen-Shannon divergence implicit in standard GAN training with alternative metrics, such as f-divergences (Nowozin et al., 2016) or Wasserstein divergences (Arjovsky et al., 2017). Much of this work is analogous to introducing various regularizers for maximum likelihood density estimation. But just as it can be difficult to choose the *right* regularizer, it can also be difficult to decide which divergence we wish to use for GAN training.

It is our contention that GANs can be improved by fully probabilistic inference. Indeed, a posterior distribution over the parameters of the generator could be broad and highly multimodal. GAN training, which is based on mini-max optimization, always estimates this whole posterior distribution over the network weights as a point mass centred on a single mode. Thus even if the generator does *not* memorize training examples, we would expect samples from the generator to be overly compact relative to samples from the data distribution. Moreover, each mode in the posterior over the network weights could correspond to wildly different generators, each with their own meaningful interpretations. By fully representing the posterior distribution over the parameters of both the generator and discriminator, we can more accurately model the true data distribution. The inferred data distribution can then be used for accurate and highly data-efficient *semi-supervised* learning.

In this paper, we present a simple Bayesian formulation for end-to-end unsupervised and semi-supervised learning with generative adversarial networks. Within this framework, we marginalize the posteriors over the weights of the generator and discriminator using stochastic gradient Hamiltonian Monte Carlo. We interpret data samples from the generator, showing exploration across several distinct modes in the generator weights. We also show data and iteration efficient learning of the true distribution. We also demonstrate state of the art semi-supervised learning performance on several benchmarks, including SVHN, MNIST, CIFAR-10, and CelebA. The simplicity of the proposed approach is one of its greatest strengths: inference is straightforward, interpretable, and stable. Indeed all of the experimental results were obtained without feature matching, normalization, or any ad-hoc techniques. And we will make code publicly available.

## 2 Bayesian GANs

Given a dataset  $\mathcal{D} = \{\mathbf{x}^{(i)}\}$  of variables  $\mathbf{x}^{(i)} \sim p_{\text{data}}(\mathbf{x}^{(i)})$ , we wish to estimate  $p_{\text{data}}(\mathbf{x})$ . We transform white noise  $\mathbf{z} \sim p(\mathbf{z})$  through a generator  $G(\mathbf{z}; \theta_g)$ , parametrized by  $\theta_g$ , to produce candidate samples from the data distribution. We use a discriminator  $D(\mathbf{x}, \theta_d)$ , parametrized by  $\theta_d$ , to output the probability that any  $\mathbf{x}$  comes from the data distribution.

Our considerations hold for general  $D$  and  $G$ , but in practice  $G$  and  $D$  are often neural networks with weight vectors  $\theta_g$  and  $\theta_d$ .

By placing distributions over  $\theta_g$  and  $\theta_d$ , we induce distributions over an uncountably infinite space of generators and discriminators, corresponding to every possible setting of these weight vectors. The generator now represents a *distribution over distributions* of data. Sampling from the induced prior distribution over data instances proceeds as follows: (1) Sample  $\theta_g \sim p(\theta_g)$ ; (2) Sample  $\mathbf{z}^{(1)}, \dots, \mathbf{z}^{(n)} \sim p(\mathbf{z})$ ; (3)  $\tilde{\mathbf{x}}^{(j)} = G(\mathbf{z}^{(j)}; \theta_g) \sim p_{\text{generator}}(\mathbf{x})$ . For posterior inference, we propose unsupervised and semi-supervised formulations in Sections 2.1 - 2.2.

We note that in an exciting recent pre-print Tran et al. (2017) briefly mention using a variational approach to marginalize weights in a GAN, as part of a general exposition on hierarchical implicit models (see also Karaletsos (2016) for a nice theoretical exploration of related topics in graphical model message passing). While promising, our approach has several key differences: (1) we use sampling to explore a full posterior over the weights, whereas Tran et al. (2017) perform a variational approximation centred on one of the modes of this posterior (and due to the properties of the KL divergence is prone to an overly compact representation of even that mode); (2) we marginalize  $\mathbf{z}$  in addition to  $\theta_g, \theta_d$ ; and (3) our representation for the posteriors is straightforward, requires no interventions, provides novel formulations for unsupervised and semi-supervised learning, and has state of the art results on many benchmarks. Conversely, Tran et al. (2017) is only pursued for fully supervised learning on a few small datasets. And their ratio estimation approach limits the size of the neural networks they can use (Tran et al., 2017), whereas in our experiments we can use comparably deep networks to maximum likelihood approaches. In the experiments we illustrate the practical value of our formulation.

Although the high level concept of a Bayesian GAN has been informally mentioned in various contexts, to the best of our knowledge we present the first detailed treatment of Bayesian GANs, with sampling based inference, and rigorous unsupervised and semi-supervised experiments.

## 2.1 Unsupervised Learning

To infer posteriors over  $\theta_g, \theta_d$ , we can iteratively sample from the following conditional posteriors:

$$p(\theta_g | \mathbf{z}, \theta_d) \propto \left( \prod_{i=1}^{n_g} D(G(\mathbf{z}^{(i)}; \theta_g); \theta_d) \right) p(\theta_g | \alpha_g) \quad (1)$$

$$p(\theta_d | \mathbf{z}, \mathbf{X}, \theta_g) \propto \prod_{i=1}^{n_d} D(\mathbf{x}^{(i)}; \theta_d) \times \prod_{i=1}^{n_g} (1 - D(G(\mathbf{z}^{(i)}; \theta_g); \theta_d)) \times p(\theta_d | \alpha_d). \quad (2)$$

$p(\theta_g | \alpha_g)$  and  $p(\theta_d | \alpha_d)$  are priors over the parameters of the generator and discriminator, with hyperparameters  $\alpha_g$  and  $\alpha_d$ , respectively.  $n_d$  and  $n_g$  are the numbers of mini-batch samples for the discriminator and generator, respectively. We define  $\mathbf{X} = \{\mathbf{x}^{(i)}\}_{i=1}^{n_d}$ .

We can intuitively understand this formulation starting from the generative process for data samples. Suppose we were to sample weights  $\theta_g$  from the prior  $p(\theta_g|\alpha_g)$ , and then condition on this sample of the weights to form a particular generative neural network. We then sample white noise  $\mathbf{z}$  from  $p(\mathbf{z})$ , and transform this noise through the network  $G(\mathbf{z};\theta_g)$  to generate candidate data samples. The discriminator, conditioned on its weights  $\theta_d$ , outputs a probability that these candidate samples came from the data distribution. Eq. (1) says that if the discriminator outputs high probabilities, then the posterior  $p(\theta_g|\mathbf{z},\theta_d)$  will increase in a neighbourhood of the sampled setting of  $\theta_g$  (and hence decrease for other settings). For the posterior over the discriminator weights  $\theta_d$ , the first two terms of Eq. (2) form a discriminative classification likelihood, labelling samples from the actual data versus the generator as belonging to separate classes. And the last term is the prior on  $\theta_d$ .

**Marginalizing the noise** In prior work, GAN updates are implicitly conditioned on a set of noise samples  $\mathbf{z}$ . We can instead marginalize  $\mathbf{z}$  from our posterior updates using Simple Monte Carlo:

$$p(\theta_g|\theta_d) = \int p(\theta_g, \mathbf{z}|\theta_d) d\mathbf{z} = \int p(\theta_g|\mathbf{z}, \theta_d) \overbrace{p(\mathbf{z}|\theta_d)}^{=p(\mathbf{z})} d\mathbf{z} \approx \frac{1}{J} \sum_{j=1}^J p(\theta_g|\mathbf{z}^{(j)}, \theta_d), \mathbf{z}^{(j)} \sim p(\mathbf{z}) \quad (3)$$

By following a similar derivation,  $p(\theta_d|\theta_g) \approx \frac{1}{J} \sum_j^J p(\theta_d|\mathbf{z}^{(j)}, \mathbf{X}, \theta_g), \mathbf{z}^{(j)} \sim p(\mathbf{z})$ .

This specific setup has several nice features for Monte Carlo integration. First,  $p(\mathbf{z})$  is a white noise distribution from which we can take efficient and exact samples. Secondly, both  $p(\theta_g|\mathbf{z}, \theta_d)$  and  $p(\theta_d|\mathbf{z}, \mathbf{X}, \theta_g)$ , when viewed as a function of  $\mathbf{z}$ , should be reasonably broad over  $\mathbf{z}$  by construction, since  $\mathbf{z}$  is used to produce candidate data samples in the generative procedure. Thus each term in the simple Monte Carlo sum typically makes a reasonable contribution to the total marginal posterior estimates. We do note, however, that the approximation will typically be worse for  $p(\theta_d|\theta_g)$  due to the conditioning on a minibatch of data in Equation 2.

By iteratively sampling from  $p(\theta_g|\theta_d)$  and  $p(\theta_d|\theta_g)$  at every step of an epoch one can, in the limit, obtain samples from the approximate posteriors over  $\theta_g$  and  $\theta_d$ . Having such samples can be very useful in practice. Indeed, one can use different samples for  $\theta_g$  to alleviate GAN collapse and generate data samples with an appropriate level of entropy. The samples for  $\theta_d$  in turn form a committee of discriminators which amplifies the overall adversarial signal, thereby further improving the unsupervised learning process. Arguably, the most rigorous method to assess the utility of these posterior samples is to examine their effect on *semi-supervised* learning, which is a focus of our experiments in Section 4.

## 2.2 Semi-supervised Learning

We extend the proposed probabilistic GAN formalism to semi-supervised learning. In the semi-supervised setting for  $K$ -class classification, we have access to a set of  $n$  unlabeled

belled observations,  $\{\mathbf{x}^{(i)}\}$ , as well as a (typically much smaller) set of  $n_s$  observations,  $\{(\mathbf{x}_s^{(i)}, y_s^{(i)})\}_{i=1}^{n_s}$ , with class labels  $y_s^{(i)} \in \{1, \dots, K\}$ . Our goal is to jointly learn statistical structure from both the unlabelled and labelled examples, in order to make much better predictions of class labels for new test examples  $\mathbf{x}_*$  than if we only had access to the labelled training inputs.

In this context, we redefine the discriminator such that  $D(\mathbf{x}^{(i)} = y^{(i)}; \theta_d)$  gives the probability that sample  $\mathbf{x}^{(i)}$  belongs to class  $y^{(i)}$ . We reserve the class label 0 to indicate that a data sample is the output of the generator. We then infer the posterior over the weights as follows:

$$p(\theta_g | \mathbf{z}, \theta_d) \propto \left( \prod_{i=1}^{n_g} \sum_{y=1}^K D(G(\mathbf{z}^{(i)}; \theta_g) = y; \theta_d) \right) p(\theta_g | \alpha_g) \quad (4)$$

$$p(\theta_d | \mathbf{z}, \mathbf{x}, \mathbf{y}_s, \theta_g) \propto \prod_{i=1}^{n_d} \sum_{y=1}^K D(\mathbf{x}^{(i)} = y; \theta_d) \prod_{i=1}^{n_g} D(G(\mathbf{z}^{(i)}; \theta_g) = 0; \theta_d) \prod_{i=1}^{n_s} (D(\mathbf{x}_s^{(i)} = y_s^{(i)}; \theta_d)) p(\theta_d | \alpha_d) \quad (5)$$

During every iteration we use  $n_g$  samples from the generator,  $n_d$  *unlabeled* samples, and all of the  $n_s$  labeled samples, where typically  $n_s \ll n$ . As in Section 2.1, we can approximately marginalize  $\mathbf{z}$  using simple Monte Carlo sampling.

Much like in the unsupervised learning case, we can marginalize the posteriors over  $\theta_g$  and  $\theta_d$ . To compute the predictive distribution for a class label  $y_*$  at a test input  $\mathbf{x}_*$  we use a model average over all collected samples with respect to the posterior over  $\theta_d$ :

$$p(y_* | \mathbf{x}_*, \mathcal{D}) = \int p(y_* | \mathbf{x}_*, \theta_d) p(\theta_d | \mathcal{D}) d\theta_d \approx \frac{1}{T} \sum_{k=1}^T p(y_* | \mathbf{x}_*, \theta_d^{(k)}), \theta_d^{(k)} \sim p(\theta_d | \mathcal{D}). \quad (6)$$

We will see that this model average is effective for boosting semi-supervised learning performance. In Section 3 we present an approach to MCMC sampling from the posteriors over  $\theta_g$  and  $\theta_d$ .

### 3 Posterior Sampling with Stochastic Gradient HMC

In the Bayesian GAN, we wish to marginalize the posterior distributions over the generator and discriminator weights, given for unsupervised learning in 2.1 and semi-supervised learning in 2.2. For this purpose, we use Stochastic Gradient Hamiltonian Monte Carlo (SGHMC) (Chen et al., 2014) for posterior sampling. The reason for this choice is threefold: (1) SGHMC is very closely related to momentum-based SGD, which we know empirically works well for GAN training; (2) we can import parameter settings (such as learning rates and momentum terms) from SGD directly into SGHMC; and most importantly, (3) many of the practical benefits of a Bayesian approach to GAN inference come from exploring a rich multimodal distribution over the weights  $\theta_g$  of the generator, which is enabled

by SGHMC, in order to fully capture the complexity and entropy of the data distribution. Alternatives, such as variational approximations, will typically centre their mass around a single mode, and thus provide a compact representation for the distribution, as well as a compact representation for that single mode, due to asymmetric biases of the KL-divergence.

The posteriors in Equations 4 and 5 are both amenable in general to HMC techniques as we can compute the gradients of the loss with respect to the parameters we are sampling. SGHMC extends HMC to the case where we use noisy estimates of such gradients in a manner which guarantees mixing in the limit of a large number of minibatches. For a detailed review of SGHMC, please see [Chen et al. \(2014\)](#). Using the update rules from Eq. (15) in [Chen et al. \(2014\)](#), we propose to sample from the posteriors over the generator and discriminator weights as in Algorithm 1.

## 4 Experiments

We evaluate our proposed Bayesian GAN (henceforth titled BayesGAN) on six benchmarks (synthetic, MNIST, CIFAR-10, SVHN, and CelebA) each with four different numbers of labelled examples. We consider multiple alternatives, including: the DCGAN ([Radford et al., 2015](#)), the recent Wasserstein GAN (W-DCGAN), an ensemble of ten DCGANs (DCGAN-10) which are formed by 10 random subsets 80% the size of the training set, and a fully supervised convolutional neural network. We also compare to the reported MNIST result for the LFVI-GAN, briefly mentioned in a recent pre-print ([Tran et al., 2017](#)), where they use fully supervised modelling on the whole dataset with a variational approximation. We interpret many of the results from MNIST in detail in Section 4.2, and find that these observations carry forward to our CIFAR-10, SVHN, and CelebA experiments.

We ran the synthetic data experiment with a 2-layer fully-connected GAN for both the generator and discriminator. For the Bayesian GAN over synthetic data we place a  $\mathcal{N}(0, I)$  on all weights and approximately integrate out  $\mathbf{z}$  using  $J = 100$  Monte-Carlo samples. We ran all other experiments with a 5-layer Bayesian deconvolutional GAN (BayesGAN) for the generative model  $G(\mathbf{z}|\theta_g)$  (see [Radford et al. \(2015\)](#) for further details about structure). The corresponding discriminator is a 5-layer 2-class DCGAN for the unsupervised GAN and a 5-layer,  $K+1$  class DCGAN for a semi-supervised GAN performing classification over  $K$  classes. The connectivity structure of the unsupervised and semi-supervised DCGANs were the same as for the BayesGAN. The networks we use are slightly different from [Salimans et al. \(2016\)](#) (e.g. we have 4 hidden layers and fewer filters per layer) so the results are also slightly different. All experiments were performed on a single TitanX GPU for consistency.

In all non-synthetic experiments we set  $J = 20$  and  $M = 1$ . For the Bayesian GAN we place a  $\mathcal{N}(0, 10I)$  prior on both the generator and discriminator weights and approximately integrate out  $\mathbf{z}$  using  $J$  Monte-Carlo samples. We run Algorithm 1 for 5000 iterations and then collect weight samples every 1000 iterations and record out-of-sample predictive

---

**Algorithm 1** One iteration of sampling for Bayesian GAN.  $\alpha$  is the friction term for SGHMC,  $\eta$  is the learning rate. We assume that the stochastic gradient discretization noise term  $\hat{\beta}$  is dominated by the main friction term (this assumption constrains us to use small step sizes). Let the number of simple MC samples be  $J$  and the number of SGHMC samples be  $M$ .

---

- Represent current posteriors with sample sets  $\{\theta_g^k\}_{k=1}^{JM}$  and  $\{\theta_d^k\}_{k=1}^{JM}$  from previous iteration

**for** number of MC iterations  $J$  **do**

- Sample minibatch of  $n_g$  noise samples  $\{\mathbf{z}^{(1)}, \dots, \mathbf{z}^{(n_g)}\}$  from noise prior  $p(\mathbf{z})$ .
- Update sample set representing  $p(\theta_g|\theta_d, \mathbf{z})$  by running SGHMC updates for  $M$  iterations:

$$\begin{aligned} \theta_g^k &\leftarrow \theta_g^k + \mathbf{v} \\ \mathbf{n} &\sim \mathcal{N}(0, 2\alpha\eta I) \\ \mathbf{v} &\leftarrow (1 - \alpha)\mathbf{v} + \eta \left( \sum_{i=1}^{n_g} \frac{\partial \log p(\theta_g|\mathbf{z}^{(i)}, \theta_d^k)}{\partial \theta_g} \right) + \mathbf{n} \end{aligned}$$

- Append  $\theta_g^k$  to sample set.

**end for**

**for** number of MC iterations  $J$  **do**

- Sample minibatch of  $n_d$  noise samples  $\{\mathbf{z}^{(1)}, \dots, \mathbf{z}^{(n_d)}\}$  from noise prior  $p(\mathbf{z})$ .
- Sample minibatch of  $n_d$  data samples  $\{\mathbf{x}^{(1)}, \dots, \mathbf{x}^{(n_d)}\}$
- Update sample set representing  $p(\theta_d|\mathbf{z}, \theta_g)$  by running SGHMC updates for  $M$  iterations:

$$\begin{aligned} \theta_d^k &\leftarrow \theta_d^k + \mathbf{v} \\ \mathbf{n} &\sim \mathcal{N}(0, 2\alpha\eta I) \\ \mathbf{v} &\leftarrow (1 - \alpha)\mathbf{v} + \eta \left( \sum_{i=1}^{n_d} \frac{\partial \log p(\theta_d|\mathbf{z}^{(i)}, \mathbf{x}^{(i)}, \theta_g^k)}{\partial \theta_d} \right) + \mathbf{n} \end{aligned}$$

- Append  $\theta_d^k$  to sample set.

**end for**

---

accuracy using Bayesian model averaging (see Eq. 6). Figure 4 contains plots of accuracy vs iteration number.

In Table 1 we summarize the semi-supervised results, where we see consistently improved performance over the alternatives. All runs are averaged over 10 random subsets of labeled examples. This gives us 10 different semi-supervised datasets, which in turn allows estimating error bars on performance (in Table 1 we show mean and 2 standard deviations). We also qualitatively illustrate the ability for the Bayesian GAN to produce complementary sets of data samples, corresponding to different representations of the generator produced by sampling from the posterior over the generator weights (Figures 1, 2, 3). We emphasize that all of the alternatives required the special techniques described in Salimans et al.

(2016) such as mini-batch discrimination and feature normalization, whereas for the results of the proposed Bayesian GAN we used none of these techniques.

## 4.1 Synthetic Dataset

We first present experiments on a simulated, multi-modal synthetic dataset as a sanity check of the basic ability to infer a multi-modal posterior  $p(\theta_g|\mathcal{D})$ . This ability not only helps avoid the collapse of the generator to a couple training examples, an instance of overfitting in regular GAN training, but also allows us to explore a set generators with different complementary properties, harmonizing together to encapsulate a rich data distribution. We generate  $D$ -dimensional synthetic data as follows:

$$\mathbf{z} \sim \mathcal{N}(0, 10 * I_d), \quad \mathbf{A} \sim \mathcal{N}(0, I_{D \times d}), \quad \mathbf{x} = \mathbf{A}\mathbf{z} + \epsilon, \quad \epsilon \sim \mathcal{N}(0, 0.01 * I_D), \quad d \ll D$$

We then fit both a regular GAN and a Bayesian GAN to such a dataset with  $D = 100$  and  $d = 2$ . The generator network for both is a two-layer neural network: 10-1000-100, fully connected, with ReLU activations. We set the dimensionality of  $\mathbf{z}$  to be 10 in order for the regular GAN to converge (it does not converge when  $d = 2$ , despite the inherent dimensionality being 2!). Consistently, the discriminator network has the following structure: 100-1000-1, fully-connected, ReLU activations. Figure 1 shows that the Bayesian GAN does a much better job qualitatively in generating samples (for which we show the first two principal components), and quantitatively in terms of Jensen-Shannon divergence to the true distribution. We also see, with the help of multidimensional scaling (Borg and Groenen, 2005), that samples from the posterior over generator weights clearly form multiple clusters.

## 4.2 MNIST

MNIST is a well-understood benchmark dataset for assessing new machine learning models. It consists of 60k (50k train, 10k test) labeled images of hand-written digits. Salimans et al. (2016) showed excellent out-of-sample performance using only a small number of labeled inputs, convincingly demonstrating the importance of good generative modelling for semi-supervised learning. Here, we follow their experimental setup for MNIST.

We evaluate the Bayesian DCGAN for semi-supervised learning using  $n_s = \{20, 50, 100, 200\}$ . We see in Table 1 that the Bayesian GAN has improved accuracy over the DCGAN, the Wasserstein GAN, and even an ensemble of 10 DCGANs! It is quite remarkable that one is able to achieve almost the same level of performance with 100 labelled examples as a fully supervised method on the whole dataset of  $n = 60,000$  samples. We also show, for comparison a supervised model using  $n_s$  samples to generally underscore the practical utility of semi-supervised learning. Moreover, Tran et al. (2017) showed that a fully supervised LFVI-GAN, on the whole MNIST training set ( $\approx 60,000$  labelled examples) produces 140 classification errors – almost twice the error of our proposed Bayesian GAN approach using only  $n_s = 100$  ( $\approx 0.0002\%$ ) labelled examples! We suspect this difference

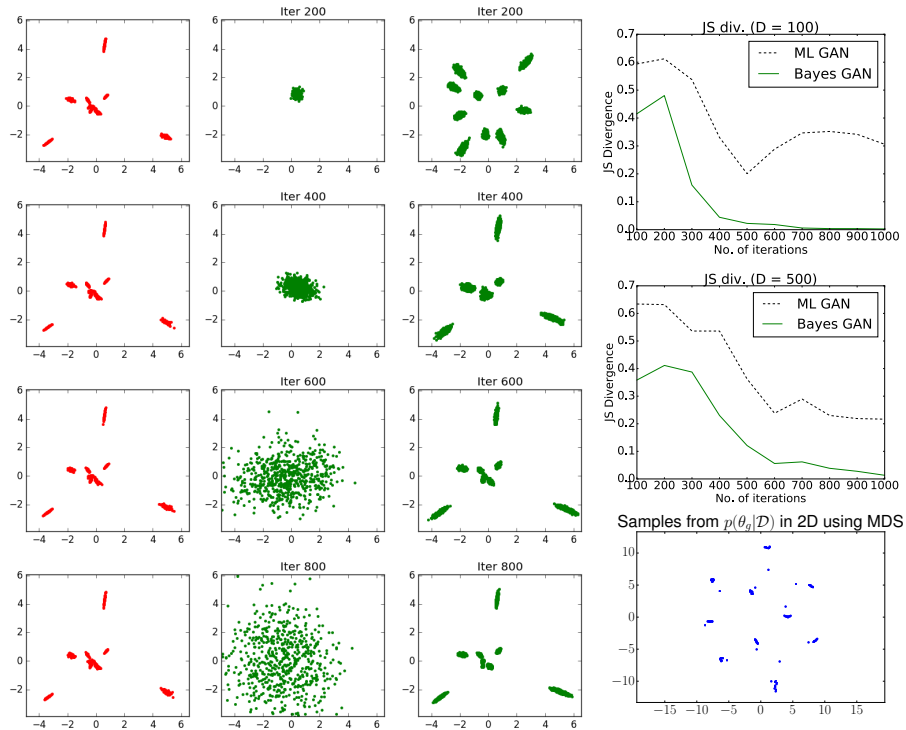


Figure 1: **Left:** Samples drawn from  $p_{\text{data}}(\mathbf{x})$  and visualized in 2-D after applying PCA. Right 2 columns: Samples drawn from  $p_{\text{MLGAN}}(\mathbf{x})$  and  $p_{\text{BGAN}}(\mathbf{x})$  visualized in 2D after applying PCA. The data is inherently 2-dimensional so PCA can explain most of the variance using 2 principal components. It is clear that the Bayesian GAN is capturing all the modes in the data whereas the regular GAN is unable to do so. **Right:** (Top 2) Jensen-Shannon divergence between  $p_{\text{data}}(\mathbf{x})$  and  $p(\mathbf{x}; \theta)$  as a function of the number of iterations of GAN training for  $D = 100$  (top) and  $D = 500$  (bottom). The divergence is computed using kernel density estimates of large sample datasets drawn from  $p_{\text{data}}(\mathbf{x})$  and  $p(\mathbf{x}; \theta)$ , after applying dimensionality reduction to 2D (the inherent dimensionality of the data). In both cases, the Bayesian GAN is far more effective at minimizing the Jensen-Shannon divergence, reaching convergence towards the true distribution, by exploring a full distribution over generator weights, which is not possible with a maximum likelihood GAN (no matter how many iterations). (Bottom) The sample set  $\{\theta_g^k\}$  after convergence viewed in 2D using Multidimensional Scaling (using Euclidean distance metric between weight samples) Borg and Groenen (2005). One can clearly see several clusters, meaning that the SGHMC sampling has discovered pronounced modes in the posterior over the weights.

largely comes from (1) the simple practical formulation of the Bayesian GAN in Section 2, (2) marginalizing  $\mathbf{z}$  via simple Monte Carlo, and (3) exploring a broad multimodal posterior distribution over the generator weights with SGHMC with our approach versus a variational approximation (prone to over-compact representations) centred on a single mode.

We can also see qualitative differences in the unsupervised data samples from our Bayesian DCGAN and the standard DCGAN in Figure 2. The top row shows sample images produced from *six* generators produced from six samples over the posterior of the generator

weights, and the bottom row shows sample data images from a DCGAN. We can see that each of the six panels in the top row have qualitative differences, almost as if a different person were writing the digits in each panel. Panel 1, for example, is quite crisp, while panel 3 is fairly thick, and panel 6 has thin and fainter strokes. By contrast, all of the data samples on the bottom row from the DCGAN are homogenous. In effect, each posterior weight sample in the Bayesian GAN corresponds to a different style, while in the standard DCGAN the style is fixed.

Moreover, practically speaking, we stress that for convergence of the maximum-likelihood DCGAN we had to resort to using tricks including minibatch discrimination, feature normalization and the addition of Gaussian noise to each layer of the discriminator. The Bayesian DCGAN needed *none* of these tricks. This robustness arises from a Gaussian prior over the weights which provides a useful inductive bias, and due to the MCMC sampling procedure which alleviates the risk of collapse and helps explore multiple modes (and uncertainty within each mode). To be balanced, we also stress that in practice the risk of collapse is not fully eliminated – indeed, some samples from  $p(\theta_g|\mathcal{D})$  still produce generators that create data samples with too little entropy. In practice, sampling is not immune to becoming trapped in sharply peaked modes. We leave further analysis for future work.

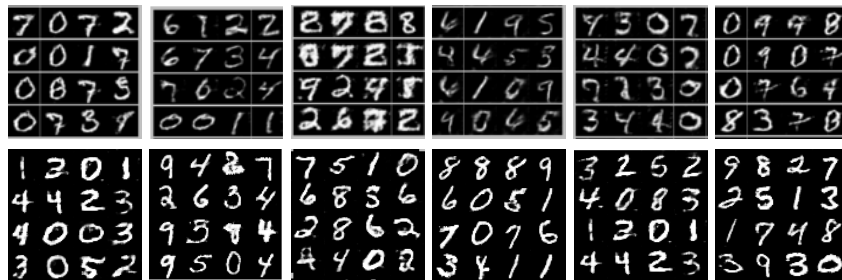


Figure 2: **Top:** Data samples from six different generators corresponding to six samples from the posterior over  $\theta_g$ . The data samples show that each explored setting of the weights  $\theta_g$  produce complementary high-fidelity samples, corresponding to different styles. The amount of variety in the samples emerges naturally using the Bayesian approach. **Bottom:** Data samples from a standard DCGAN (trained six times). By contrast, these samples are homogenous in style.

### 4.3 CIFAR-10

CIFAR-10 is also a popular benchmark dataset Krizhevsky et al. (2010), with 50k training and 10k test images. It is harder to model due the data being 32x32 RGB images of real objects. Figure 3 shows datasets produced from four different generators corresponding to samples from the posterior over the generator weights. As with MNIST, we see meaningful qualitative variation between the panels. In Table 1 we also see again (but on this more challenging dataset) that using Bayesian GANs as a generative model within the semi-supervised learning setup significantly decreases test set error over the alternatives, especially when  $n_s \ll n$ .

Table 1: Detailed supervised and semi-supervised learning results for all datasets. In almost all experiments BayesGAN outperforms DCGAN and W-DCGAN significantly, and typically even outperforms ensembles of DCGANs. The total runtimes, per *epoch*, in minutes, are provided in rows including the dataset name. While all experiments were performed on a single GPU, note that DCGAN-10 and BayesGAN methods can be sped up straightforwardly using multiple GPUs. Results are averaged over 10 partitions of the data  $\pm 2$  stdev.

$n_s$	No. of misclassifications for MNIST. Test error rate for others.				
	Supervised	DCGAN	W-DCGAN	DCGAN-10	BayesGAN
MNIST	$N=60k, D = (28, 28)$	14	15	114	153
20	—	$1823 \pm 412$	$1687 \pm 387$	$1087 \pm 564$	<b><math>997 \pm 348</math></b>
50	—	$453 \pm 110$	$490 \pm 170$	$189 \pm 103$	<b><math>154 \pm 89</math></b>
100	$2134 \pm 525$	$128 \pm 11$	$156 \pm 17$	$97 \pm 8.2$	<b><math>89 \pm 3.4</math></b>
200	$1389 \pm 438$	$95 \pm 3.2$	$91 \pm 5.2$	<b><math>78 \pm 2.8</math></b>	$79 \pm 1.4$
CIFAR10	$N=50k, D = (32, 32, 3)$	18	19	146	205
1000	$63.4 \pm 2.6$	$58.2 \pm 2.8$	$57.1 \pm 2.4$	$31.1 \pm 2.5$	<b><math>29.7 \pm 3.2</math></b>
2000	$56.1 \pm 2.1$	$47.5 \pm 4.1$	$49.8 \pm 3.1$	$29.2 \pm 1.2$	<b><math>25.4 \pm 4.3</math></b>
4000	$51.4 \pm 2.9$	$40.1 \pm 3.3$	$38.1 \pm 2.9$	$27.4 \pm 3.2$	<b><math>22.8 \pm 2.4</math></b>
8000	$47.2 \pm 2.2$	$29.3 \pm 2.8$	$27.4 \pm 2.5$	$25.5 \pm 2.4$	<b><math>20.9 \pm 1.8</math></b>
SVHN	$N=75k, D = (32, 32, 3)$	29	31	217	322
500	$53.5 \pm 2.5$	$31.2 \pm 1.8$	$29.4 \pm 1.8$	$27.1 \pm 2.2$	<b><math>26.7 \pm 2.8</math></b>
1000	$37.3 \pm 3.1$	$25.5 \pm 3.3$	$25.1 \pm 2.6$	$18.3 \pm 1.7$	<b><math>14.1 \pm 2.3</math></b>
2000	$26.3 \pm 2.1$	$22.4 \pm 1.8$	$23.3 \pm 1.2$	$16.7 \pm 1.8$	<b><math>14.0 \pm 1.4</math></b>
4000	$20.8 \pm 1.8$	$20.4 \pm 1.2$	$19.4 \pm 0.9$	$14.0 \pm 1.4$	<b><math>9.8 \pm 1.1</math></b>
CelebA	$N=100k, D = (50, 50, 3)$	103	98	649	1134
1000	$53.8 \pm 4.2$	$52.3 \pm 4.2$	$51.2 \pm 5.4$	$47.3 \pm 3.5$	<b><math>43.9 \pm 2.9</math></b>
2000	$36.7 \pm 3.2$	$37.8 \pm 3.4$	$39.6 \pm 3.5$	$31.2 \pm 1.8$	<b><math>30.8 \pm 2.3</math></b>
4000	$34.3 \pm 3.8$	$31.5 \pm 3.2$	$30.1 \pm 2.8$	$29.3 \pm 1.5$	<b><math>25.4 \pm 1.3</math></b>
8000	$31.1 \pm 4.2$	$29.5 \pm 2.8$	$27.6 \pm 4.2$	$26.4 \pm 1.1$	<b><math>22.3 \pm 1.8</math></b>

#### 4.4 SVHN

The StreetView House Numbers (SVHN) dataset consists of RGB images of house numbers taken by StreetView vehicles. Unlike MNIST, the digits significantly differ in shape and appearance. The experimental procedure closely followed that for CIFAR-10. There are approximately 75k training and 25k test images. We see in Table 1 a particularly pronounced difference in performance between BayesGAN and the alternatives. Data samples are shown in Figure 3.

#### 4.5 CelebA

The large CelebA dataset contains 120k celebrity faces amongst a variety of backgrounds (100k training, 20k test images). To reduce background variations we used a standard face detector Viola and Jones (2004) to crop the faces into a standard  $50 \times 50$  size, which is actually larger than most applications of GANs in the literature. Figure 3 shows data samples from the trained Bayesian GAN. In order to assess performance for semi-supervised learn-

ing we created 32-class classification task by predicting a 5-bit vector indicating whether or not the face: is blond, has glasses, is male, is pale and is young. Table 1 shows the same pattern of promising performance for CelebA.

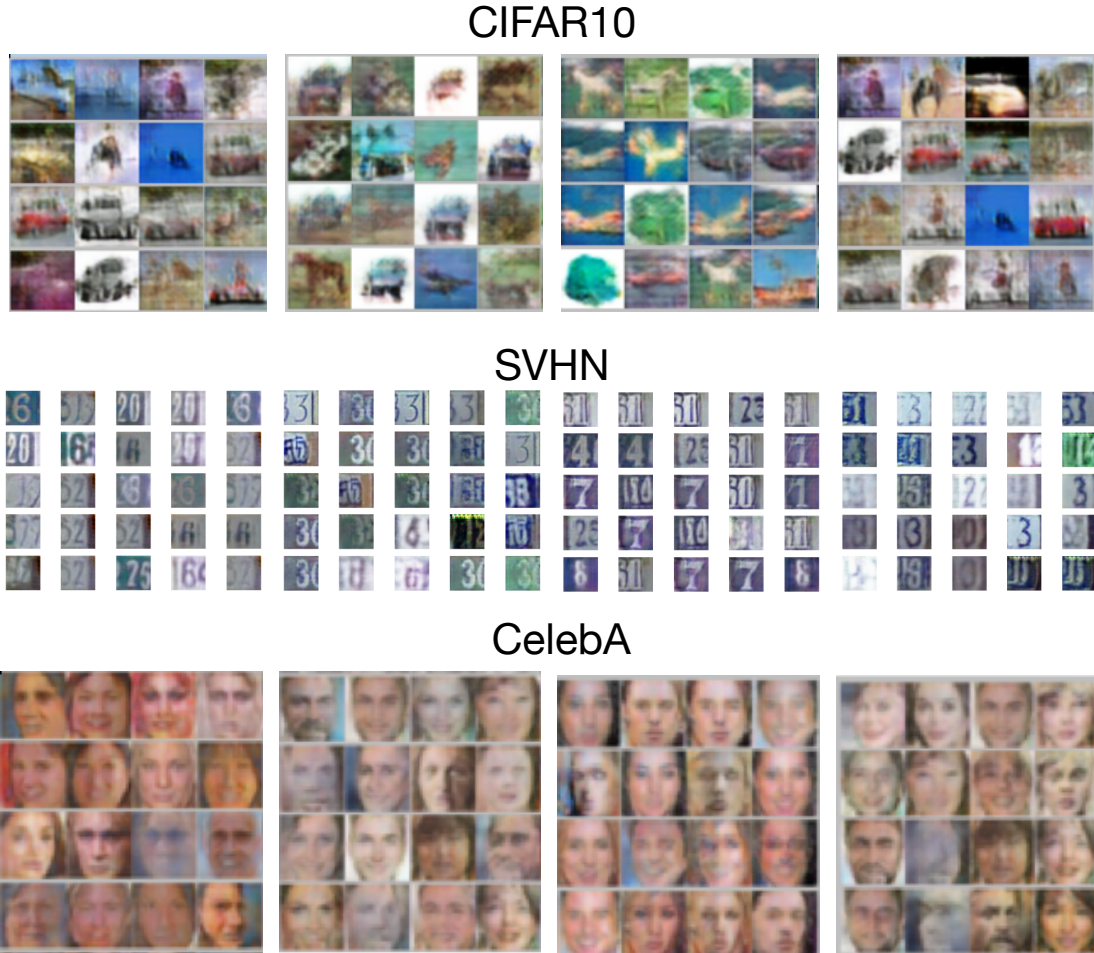


Figure 3: Data samples for the CIFAR10, SVHN and CelebA datasets from four different generators created using four different samples from the posterior over  $\theta_g$ . Each panel corresponding to a different  $\theta_g$  has different qualitative properties, showing the complementary nature of the different aspects of the distribution learned using a fully probabilistic approach.

## 5 Discussion

By exploring rich multimodal distributions over the weight parameters of the generator, the Bayesian GAN can capture a diverse set of complementary and interpretable representations of data. We have shown that such representations can enable state of the art performance on semi-supervised problems, using a simple inference procedure.

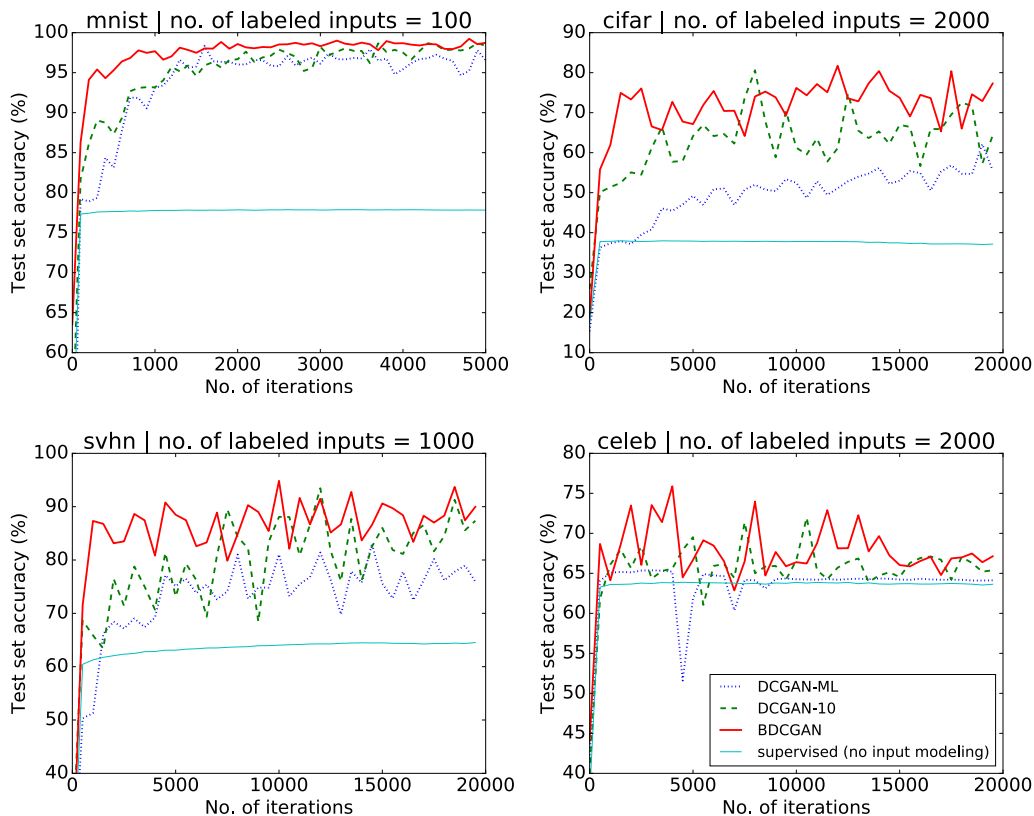


Figure 4: Test accuracy as a function of iteration number. We can see that after about 1000 SG-HMC iterations, the sampler is mixing reasonably well. We also see that per iteration the SG-HMC sampler is learning the data distribution more efficiently than the alternatives.

Effective semi-supervised learning of natural high dimensional data is crucial for reducing the dependency of deep learning on large labelled datasets. Often labeling data is not an option, or it comes at a high cost – be it through human labour or through expensive instrumentation (such as LIDAR for autonomous driving). Moreover, semi-supervised learning provides a practical and quantifiable mechanism to benchmark the many recent advances in unsupervised learning.

In the future, one could estimate the marginal likelihood of a probabilistic GAN, having integrated away distributions over the parameters. The marginal likelihood provides a natural utility function for automatically learning hyperparameters, and for performing model comparison between different GAN architectures. One could also investigate a variety of divergence measures (such as the family of  $\alpha$ -divergences) for deterministic approximate inference, to promote entropy in samples. It would also be interesting to consider the Bayesian GAN in conjunction with a non-parametric Bayesian deep learning framework, such as deep kernel learning (Wilson et al., 2016a,b). We hope that our work will help inspire continued exploration into Bayesian deep learning.

**Acknowledgements** We thank Soumith Chintala for helpful advice.

## References

- M. Arjovsky, S. Chintala, and L. Bottou. Wasserstein GAN. *arXiv preprint arXiv:1701.07875*, 2017.
- I. Borg and P. J. Groenen. *Modern multidimensional scaling: Theory and applications*. Springer Science & Business Media, 2005.
- T. Chen, E. Fox, and C. Guestrin. Stochastic gradient Hamiltonian Monte Carlo. In *Proc. International Conference on Machine Learning*, June 2014.
- I. Goodfellow, J. Pouget-Abadie, M. Mirza, B. Xu, D. Warde-Farley, S. Ozair, A. Courville, and Y. Bengio. Generative adversarial nets. In *Advances in neural information processing systems*, pages 2672–2680, 2014.
- T. Karalestos. Adversarial message passing for graphical models. *arXiv preprint arXiv:1612.05048*, 2016.
- D. P. Kingma and M. Welling. Auto-encoding variational Bayes. *arXiv preprint arXiv:1312.6114*, 2013.
- A. Krizhevsky, V. Nair, and G. Hinton. Cifar-10 (Canadian institute for advanced research). 2010. URL <http://www.cs.toronto.edu/~kriz/cifar.html>.
- S. Nowozin, B. Cseke, and R. Tomioka. f-GAN: Training generative neural samplers using variational divergence minimization. In *Advances in Neural Information Processing Systems*, pages 271–279, 2016.
- A. Radford, L. Metz, and S. Chintala. Unsupervised representation learning with deep convolutional generative adversarial networks. *arXiv preprint arXiv:1511.06434*, 2015.
- T. Salimans, I. J. Goodfellow, W. Zaremba, V. Cheung, A. Radford, and X. Chen. Improved techniques for training gans. *CoRR*, abs/1606.03498, 2016. URL <http://arxiv.org/abs/1606.03498>.
- D. Tran, R. Ranganath, and D. M. Blei. Deep and hierarchical implicit models. *CoRR*, abs/1702.08896, 2017. URL <http://arxiv.org/abs/1702.08896>.
- P. Viola and M. J. Jones. Robust real-time face detection. *Int. J. Comput. Vision*, 57(2): 137–154, May 2004. ISSN 0920-5691. doi: 10.1023/B:VISI.0000013087.49260.fb. URL <http://dx.doi.org/10.1023/B:VISI.0000013087.49260.fb>.
- A. G. Wilson, Z. Hu, R. Salakhutdinov, and E. P. Xing. Deep kernel learning. *Artificial Intelligence and Statistics*, 2016a.
- A. G. Wilson, Z. Hu, R. R. Salakhutdinov, and E. P. Xing. Stochastic variational deep kernel learning. In *Advances in Neural Information Processing Systems*, pages 2586–2594, 2016b.

## Appendix

In this Appendix, we show further samples from the Bayesian GAN generator.



Figure 5: A larger set of data samples for CIFAR10 from four different generators created using four different samples from the posterior over  $\theta_g$ . Each panel corresponding to a different  $\theta_g$  has different qualitative properties, showing the complementary nature of the different aspects of the distribution learned using a fully probabilistic approach.



Figure 6: A larger set of data samples for SVHN from four different generators created using four different samples from the posterior over  $\theta_g$ . Each panel corresponding to a different  $\theta_g$  has different qualitative properties, showing the complementary nature of the different aspects of the distribution learned using a fully probabilistic approach.

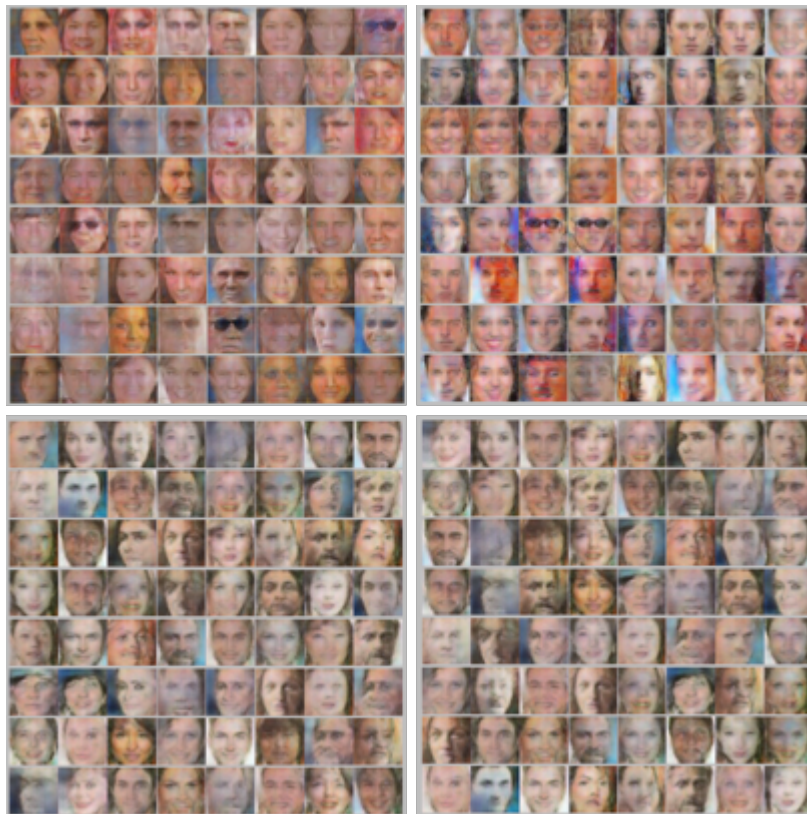


Figure 7: A larger set of data samples for CelebA from four different generators created using four different samples from the posterior over  $\theta_g$ . Each panel corresponding to a different  $\theta_g$  has different qualitative properties, showing the complementary nature of the different aspects of the distribution learned using a fully probabilistic approach.